Aurora on Ganymede

Melissa A. McGrath,[1] Xianzhe Jia,[2] Kurt Retherford,[3] Paul D. Feldman,[4]
Darrell F. Strobel,[4] and Joachim Saur[5]

Received 27 August 2012; revised 8 January 2013; accepted 9 January 2013; published 17 May 2013.

[1] We present four sets of ultraviolet images of Ganymede acquired with the Hubble Space Telescope (HST) from 1998 to 2007, all of which show auroral emission from electron excited atomic oxygen. The three different hemispheres of Ganymede captured in the observations show strikingly different emission morphologies. Ultraviolet emission at 1356 Å is brightest at relatively high latitude on the orbital trailing (upstream plasma) hemisphere and in an auroral oval that extends to as low as ~10°N latitude on the orbital leading (downstream plasma) hemisphere. Two sets of images of the Jupiter-facing hemisphere acquired at nearly the same sub-Earth longitude but separated by ~4 years show very similar emission morphology that is consistent with the pattern of emission seen in the upstream and downstream images: the emission is at high latitude in the upstream quadrant and at low latitude in the downstream quadrant. This implies that the large-scale, nominal "auroral oval" on Ganymede is apparently quite stable with time, despite significant brightness fluctuations within the overall stable pattern during the 10–30 min time scale between individual images. The overall emission morphology appears to be driven primarily by the strong Jovian magnetospheric plasma interaction with Ganymede and does not appear to be strongly influenced by the orientation of the background Jovian magnetic field. The observed auroral oval pattern is reasonably well matched by a magnetohydrodynamic (MHD) model optimized to fit the Galileo magnetic field measurements near Ganymede. The location of the auroral oval from these data provides a reasonable match to the location of the well-defined visible boundary of the Ganymede polar cap except in the northern, leading hemisphere.

Citation: McGrath, M. A., X. Jia, K. Retherford, P. D. Feldman, D. F. Strobel, and J. Saur (2013), Aurora on Ganymede, *J. Geophys. Res. Space Physics*, *118*, 2043–2054, doi:10.1002/jgra.50122.

1. Introduction

[2] One of the most dramatic results of the Galileo mission to the Jupiter system was the discovery of an intrinsic magnetic field associated with Jupiter's largest satellite Ganymede [*Kivelson et al*., 1996, 1997], making it the only known satellite with a "magnetosphere within a magnetosphere" in our solar system. This discovery was reinforced by contemporaneous spectroscopic observations with the Hubble Space Telescope (HST) of atomic oxygen emission associated with the polar regions of the satellite [*Hall et al*., 1998] and the subsequent stunning ultraviolet images obtained in 1998 that revealed unambiguous polar auroral emission from Ganymede with brightness of up to 300 Rayleighs (R) in localized spots [*Feldman et al*., 2000]. These images also show a diffuse background emission of ≤50 R across the rest of the disk of the satellite. The oxygen emission is thought to be produced primarily by electron dissociative excitation of the molecular oxygen that dominates Ganymede's tenuous atmosphere [*Hall et al*., 1998], although there is also likely a lesser contribution from electron excitation of the atomic oxygen component of the atmosphere. The tenuous atmosphere is produced by sputtering of Ganymede's icy surface by the Jovian magnetospheric plasma within which it orbits [*Johnson et al*., 1982].

[3] The Jovian magnetospheric plasma at Ganymede is characterized by a thermal component with $n_e \sim 5$–$20\,\mathrm{cm}^{-3}$, $T_e \sim 20\,\mathrm{eV}$ plus a superthermal component with $n_e \sim 0.5$–$2\,\mathrm{cm}^{-3}$, $T_e \sim 2\,\mathrm{keV}$ [*Scudder et al*., 1981]. The plasma is confined by Jupiter's magnetic field and slightly subcorotates at $v \sim 150\,\mathrm{km/s}$. By contrast, the satellite is in a phase-locked orbit around Jupiter with an orbital velocity of ~11 km/s, meaning that the bulk plasma flow is constantly overtaking the satellite. Like the other Galilean satellites, Ganymede therefore has "leading" and "trailing" orbital hemispheres, which correspond to the downstream and upstream directions relative to the bulk plasma flow. We therefore use the terms leading/downstream and trailing/upstream interchangeably throughout the rest of the paper. At Ganymede's distance from Jupiter, the plasma is confined to a low scale height current sheet (also called the plasma sheet) centered roughly around the Jovian magnetic equator [*Khurana et al*., 2004, 2007]. Because of the 10° tilt of the Jupiter magnetic field to its

[1]NASA Marshall Space Flight Center, Huntsville, Alabama, USA.
[2]University of Michigan, Ann Arbor, Michigan, USA.
[3]Southwest Research Institute, San Antonio, Texas, USA.
[4]Johns Hopkins University, Baltimore, Maryland, USA.
[5]University of Cologne, Cologne, Germany.

Corresponding author: Melissa A. McGrath, NASA Marshall Space Flight Center. (melissa.a.mcgrath@nasa.gov)

2169-9380/13/10.1002/jgra.50122

rotational axis, the current sheet oscillates up and down with an ~5 h period at the satellite.

[4] The thermal component of the Jovian plasma at Ganymede can produce a maximum of only ~10–40 R, which rules it out as the main the source of either the diffuse or the bright spot auroral emissions [*Eviatar et al*., 2001]. *Eviatar et al*. also estimated the electron densities and temperatures at Ganymede required to produce the peak auroral emission intensity. Because the Ganymede atmosphere is so tenuous, direct impact excitation by the energetic electrons observed with the Galileo spacecraft at Ganymede [*Gurnett et al*., 1996; *Williams et al*., 1997a, 1997b; *Paranicas et al*., 1999] is an inefficient process, with a low excitation rate due to the low density and decreasing collision cross section with increasing energy [see *Eviatar et al*., 2001, Figure 3]. Extrapolating the energetic electron density using the magnetic field magnitude, *Eviatar et al*. estimated a surface density of $n_e \sim 300\,\mathrm{cm}^{-3}$. The observed 300 R intensity can then be produced only if the entire electron population is characterized by a Maxwellian distribution with temperature in the range of 75–300 eV. These calculations showed that the bulk of the electrons producing both the diffuse background and the bright spots must be locally accelerated. *Eviatar et al*. [2001] proposed two possible local acceleration mechanisms, stochastic acceleration by electrostatic waves, and an acceleration process analogous to that on Earth whereby magnetic field-aligned electric fields develop in the presence of sufficiently intense field-aligned currents. The location of the brightest emission in the *Feldman et al*. [2000] images seems to be consistent with the location of the boundary between Ganymede's open and closed magnetic field lines (the "separatrix"), where local acceleration by field-aligned electric fields would be plausible.

[5] We present three previously unpublished sets of HST UV images of Ganymede taken in 2000, 2003, and 2007, in addition to the original 1998 UV images published previously by *Feldman et al*. [2000] and *Eviatar et al*. [2001]. A summary of the observations used in this paper is given in Table 1; a schematic diagram showing the geometry of the observations is included in Figure 1. Two of the four data sets were acquired either when Ganymede was in Jupiter shadow (eclipse), or just prior to Ganymede entry into Jupiter shadow, covering (approximately) the Jupiter-facing hemisphere of the satellite; a third set covers Ganymede's leading/downstream hemisphere; and the original 1998 data set covers Ganymede's trailing/upstream hemisphere. Combination of these images allows a nearly complete mapping of the location (latitude and longitude) of Ganymede's auroral ovals. For terrestrial auroral emissions,

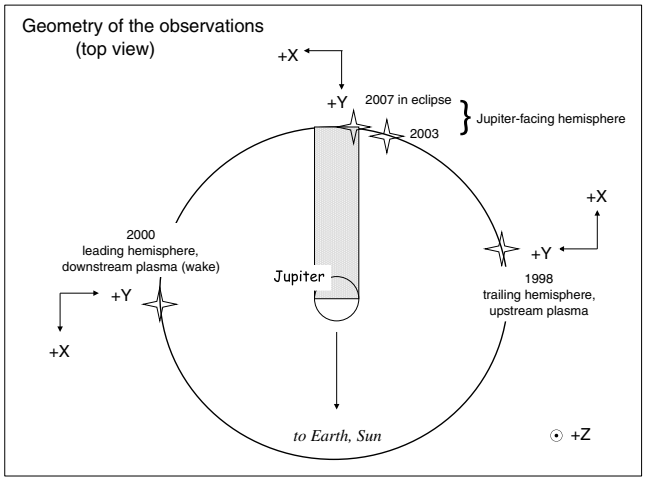

Figure 1. Geometry of the four sets of observations presented in this paper. Further details are provided in Table 1. The $+X$ axis is parallel to the plasma flow; the $+Y$ axis points to Jupiter. The $+Z$ axis is out of the page, parallel to the Jupiter and Ganymede rotation axes. This convention is used throughout the figures in the rest of the paper.

Table 1. Summary of Observations[a]

							Subobserver			
Program	**Orbit**	**Exposure ID**	**Inst/Config**	**Date**	**Start Time (UT)**	**Exp Time (s)**	**Long**	**Lat**	**Sys III**	**Size**
HST 7939	1	o53k01010	STIS/G140L	30 Oct 1998	08:21	850	290	1.7	230	1.71
		o53k01020			08:39	850	290		240	
	2	o53k01030			09:40	1205	292		276	
		o53k01040			10:07	1205	293		292	
	3	o53k01050			11:17	1125	296		331	
		o53k01060			11:43	1100	297		346	
	4	o53k01070			12:54	1200	299		27	
		o53k01080			13:17	1130	300		40	
HST 8224	1	o5d602010	STIS/G140L	23 Dec 2000	03:45	740	105	3.0	264	1.75
		o5d602020			04:01	740	105		273	
	2	o5d602030			05:01	1100	107		309	
		o5d602040			05:26	1100	108		323	
HST 9296	1	o8m301010	STIS/G140L	30 Nov 2003	20:49	820	336	−1.3	220	1.33
		o8m301020			21:06	820	337		231	
	2	o8m301030			22:10	1100	339		271	
		o8m301040			22:35	1100	340		288	
HST 10871	1	j9pn11cgq X	ACS/F125LP	25 Feb 2007	10:30	600	349 p	−3.0	39	1.33
		j9pna1chq			10:45	600	350 e		48	
		j9pna1ciq			10:56	600	351 e		54	
		j9pna1cjq X			11:06	600	351 e		60	

[a]X, image not used in this analysis; p, Ganymede in partial Jupiter eclipse; e, Ganymede in Jupiter eclipse.

there is a correspondence between the UV auroral oval and the electron precipitation location [*Eviatar et al*., 2001]. Several recent models predict the location of the boundary between open and closed magnetic field lines on Ganymede, which in analogy with Earth is an expected place to find magnetic field–aligned electric fields that can cause local acceleration of charged particles. The newly available Ganymede auroral ovals and existing models have motivated us to compare the two for the first time.

2. Description of the Observations

[6] We analyze four sets of HST UV observations of Ganymede acquired with the Space Telescope Imaging Spectrograph (STIS) in 1998, 2000, and 2003 and with the Advanced Camera for Surveys (ACS) in 2007. The 1998 data were first published by *Feldman et al*. [2000] and have also been presented and discussed by *Eviatar et al*. [2001] and *McGrath et al*. [2004]. Two images were acquired in each of four HST orbits in the 1998 observations, two images in each of two orbits were acquired in the 2000 and 2003 observations, and four images were acquired in one orbit in the 2007 ACS observations. Further details about the observations are given in Table 1.

[7] Because of the low signal-to-noise ratio (S/N) of the individual images, we have chosen in this analysis of the auroral emission morphology to sum all the images for each observing date and concentrate on the gross, overall large-scale pattern of the emission. The shortest exposure times for the individual images is 10 min, so it is not possible to extract short time scale temporal variability from these data. The low S/N of 1–2 in the individual images, the small number of orbits for each observing date, and the ~30 min data gap between HST orbits further limit our ability to perform meaningful temporal analysis on these data. Summing the images from each observing date means that we do not attempt to identify changes due to the 10-h rotation period of Jupiter's magnetic field, and therefore, the 5-h period of the plasma sheet relative to Ganymede. Coverage of significantly less than a full 10-h period in three of the four data sets would make identifying such effects challenging. While there is clearly variability on the shorter minutes to hours time scales [see, e.g., *Eviatar et al*., 2001, Figure 1], inspection of the individual images, as well as summing the images from each orbit instead of each observing date, seems to indicate that the shorter–time scale changes are characterized more by fluctuations in the brightness of the localized bright regions within a relatively stable overall pattern, instead of large changes in the spatial locations of the localized bright regions. Another way of saying this is that, at any given longitude, the latitude of the brightest emission does not change significantly, but its brightness sometimes does. The spatial changes are often subtle and are the subject of an ongoing analysis [*Saur et al*., 2011] using a newer (not yet publicly available), longer time coverage data set designed to look for changes due to the location of Ganymede relative to the plasma sheet. Our analysis is therefore limited to discerning how the auroral emission pattern changes among the different hemispheres of the satellite and over a multiyear time scale.

[8] The three sets of STIS observations were acquired with an identical instrument setup using grating G140L covering the wavelength range of 1150–1729 Å with the long slit ($52'' \times 2''$, which is limited in the spatial direction by the $25'' \times 25''$ size of the detector). The STIS MAMA detector has 1024×1024 pixels of $0.025''$ size. This instrument setup produces a two dimensional dispersed image of Ganymede with both a surface-reflected light continuum and, at wavelengths where there is emission, a monochromatic image of the satellite. The raw data format is well illustrated by *Feldman et al*. [2000, Figure 1]. In this paper, we focus exclusively on the images of Ganymede in the atomic oxygen emission line at 1356 Å, where the surface reflected light and geocoronal background emission are minimal. We use the standard pipeline calibrated data, which has been flat-fielded, corrected for geometric distortion, and converted to absolute flux. To maximize S/N ratio, the STIS images are also rebinned to 512×512 pixels, which results in a rebinned pixel size of $0.05''$, providing spatial resolution of ~75–100 km at Ganymede. We subtract off the detector background signal using image rows immediately above and below the Ganymede spectrum. The location of Ganymede can be determined very precisely (to 1 px accuracy) in the spatial (y) direction using the reflected light continuum and in the dispersion (x) direction using the known slit width and the known wavelengths of the prominent geocoronal emissions at H I Lyman-α (1215.7 Å) and O I 1304 Å, which fill the slit. An identical data reduction process is used for all STIS data sets, producing a uniformly reduced and calibrated set of images that can be quantitatively compared.

[9] The ACS data were acquired using the F125LP filter and the Solar Blind Camera (SBC) just prior to and while Ganymede was in Jupiter shadow. The F125LP filter does not have adequate "red leak" suppression to compensate for the much higher longer wavelength flux from Ganymede at visible wavelengths. Therefore, to get usable UV images, the data need to be acquired when Ganymede is in Jupiter shadow, when there is no visible reflected solar light present. Of the four images acquired with the ACS in a single HST orbit, the first image is not usable for studying the auroral oxygen emission because Ganymede is still partly in sunlight; however, this image provides precise information on the location of Ganymede in the field of view, information that is difficult or impossible to determine from the images acquired in Jupiter shadow. The fourth image is dominated by Jupiter scattered light because of Ganymede's proximity to the planet, with no Ganymede signal apparent. We therefore use only the second and third images of the ACS data set. Unlike the STIS spectral images, the ACS F125LP filter throughput includes emission from both the O I 1304 and 1356 Å oxygen lines. The ACS SBC detector has rectangular ($0.034'' \times 0.03''$) instead of square pixels. The ACS data have therefore first been resampled to a grid with square $0.034'' \times 0.034''$ pixels before being rebinned by a factor of 2, resulting in somewhat lower spatial resolution than the STIS images. A detector background from areas adjacent to the Ganymede emission image has been subtracted from the data.

[10] For both STIS and ACS images, we extract a square region centered on the oxygen 1356 Å emission and rotate it so that Jupiter North is up in all the figures in this paper. We produce a single composite image for each observing date by summing all of the images, except for the ACS data as noted above. A 3-point running boxcar smoothing is applied to each image. Finally, we superpose a latitude-longitude grid using the known size and location of

Ganymede, and then overlay brightness contours in units of Rayleighs (R) on each image.

3. Emission Morphology

[11] Figure 2 shows the four composite images from the four observing dates. Generally speaking Ganymede's auroral emission is characterized by localized bright regions with peak brightnesses of ~100–400 R in the composite images. The location of the brightest emission varies noticeably among the three hemispheres of the satellite imaged on the different dates, with the brightest emission occurring at significantly higher latitude on the trailing/upstream hemisphere than on the leading/downstream hemisphere. A more quantitative evaluation of this is provided in Figure 3, where the location (latitude, longitude) of the brightest emission from the composite images is shown in both normal cylindrical and polar projections. For the STIS images (1998, 2000, 2003), the error in the location of the peak emission has been determined by comparing the locations of the bright regions among four independent reductions of the same data sets. This error is due to the ~1 pixel uncertainty in locating the center of Ganymede in both the detector x and y directions. For example, our Figure 2 shows the images previously published by *Feldman et al.* [2000, Figure 3] and *Eviatar et al.* [2001, Figure 1]. The independent analyses of the STIS data sets show a conservative uncertainty of ~5° in the position of the peak emission. The uncertainty is larger (~10°) for the ACS eclipse images, due to the larger uncertainty in locating the disk of Ganymede in the preeclipse image. To assess this uncertainty, we have carefully compared two independent reductions done by M. McGrath and K. Retherford to produce the error bars used in Figure 3.

[12] Inspection of the composite images and the plots shown in Figure 3 reveal that on the trailing/upstream hemisphere (centered on 270°W longitude), the brightest emission occurs at relatively high latitude (~40°–55° latitude), while on the leading/downstream hemisphere it occurs approximately 20°–30° lower in latitude (at ~10°–30° latitude). The intermediate (Jupiter-facing) hemisphere shows a similar pattern from a different vantage point, where the brightest emission appears to bridge between the latitude of the emission observed on the upstream and downstream hemispheres, that is, emission is at higher latitude in the upstream quadrant (270°W–360°W), and significantly lower latitude in the downstream quadrant (360°W–90°W longitude). The Jupiter-facing hemisphere morphology is remarkably similar (although not identical) in the 2003 STIS images and the 2007 ACS images, indicating that the gross overall pattern of the Ganymede auroral emission is relatively stable on a multiyear time scale. This point is further supported by the fact that in regions that are common among the four images, the location of the emission almost always overlaps, and sometimes very closely, e.g., ~15°W–60°W longitude in the northern hemisphere there is remarkable agreement in the location of the auroral emission from the 2000, 2003, and 2007 images. In regions where the emission has been mapped, there is only one region where the emission location from different dates does not overlap within the error bars, ~345°W–360°W longitude in the southern hemisphere.

[13] Figures 2 and 3 also reveal that the auroral emission is not symmetric about the equator in the N-S direction in any of the four sets of images. In the trailing/upstream hemisphere, the brightest band of emission is at higher latitude in the north than in the south (~45°N–60°N from

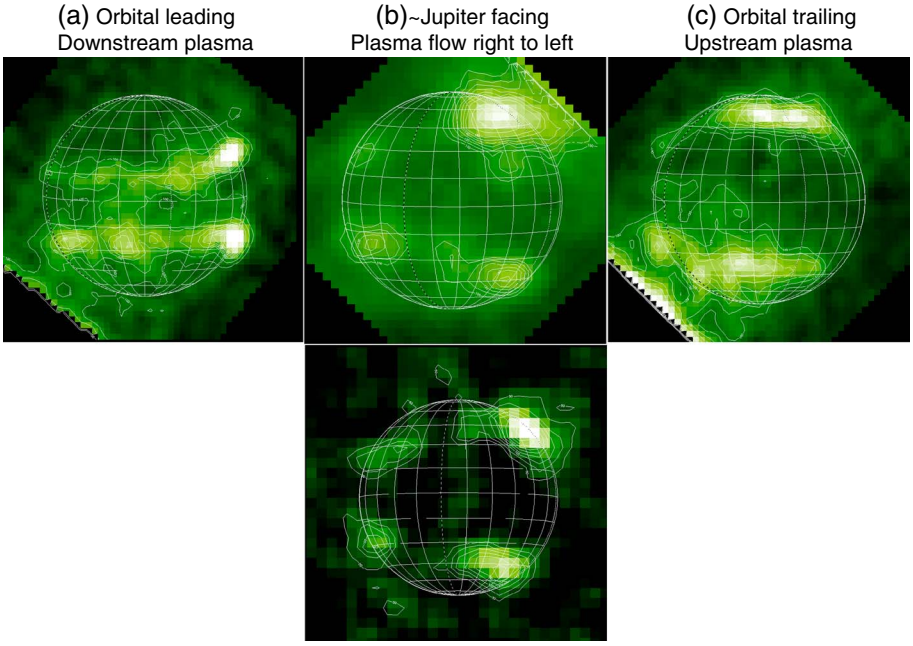

Figure 2. Ganymede auroral emission from atomic oxygen illustrating the different morphologies on the different hemispheres of the satellite. The magnetospheric plasma flow is into the page for the trailing hemisphere, out of the page for the leading hemisphere, and approximately from right to left for the Jupiter-facing hemisphere. The black and white dashed line in each image represents the 0°W (2003 and 2007), 90°W (2000), or 270°W (1998) longitude meridian.

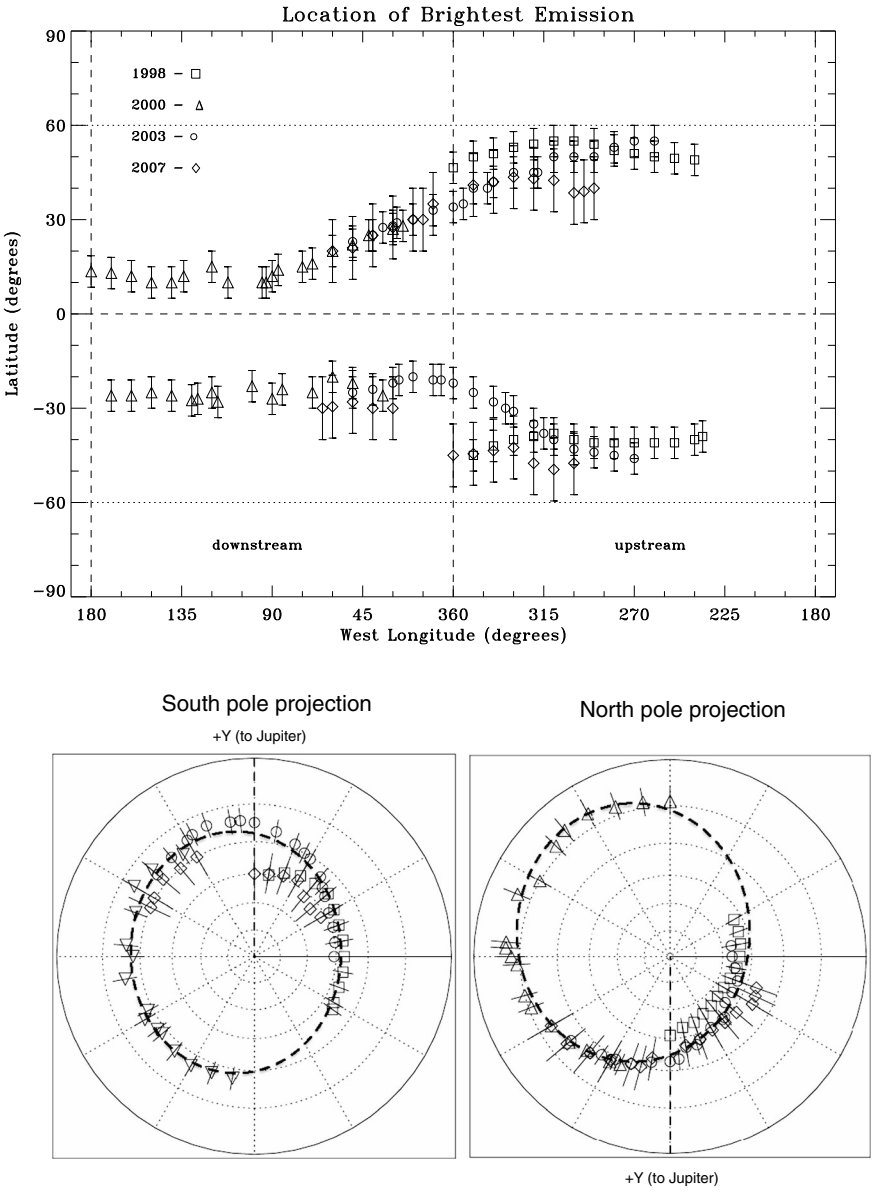

Figure 3. Cylindrical (top) and polar (bottom) projections of the latitude and longitude of the peak auroral emission brightness from the composite images shown in Figure 2. The dark line is in the *X* (plasma flow) direction at longitude 270°, the center of the trailing/upstream hemisphere, and the dotted line is at longitude 360°, the center of the Jupiter-facing hemisphere. The polar projections emphasize the degree to which the auroral emission is stretched in the downstream and anti-Jupiter direction and the fact that the emission is not symmetric around the plasma flow axis or symmetric between northern hemisphere and southern hemisphere. Different symbols are used for the different dates, as indicated in the legend at the top. The same symbols are used for these dates in all subsequent figures.

~255°W–300°W, but ~30°S–45°S from ~300°W–330°W), but the opposite is true on the leading hemisphere, where it is at lower latitude in the north than in the south. The emission pattern also shows less variation with longitude in the south than the north, especially between 0° and 90°W longitude. For the Jupiter-facing hemisphere, the emission is at lower latitude in the southern compared to the northern hemisphere in the 2003 STIS composite image, but opposite in the 2007 composite image.

[14] The polar projection plots of the emission shown in Figure 3 provide another way of understanding the emission pattern described above. What we might call Ganymede's nominal "auroral oval" is compressed to higher latitude in the upstream direction and stretched to lower latitude in the downstream (wake) direction, as expected from the strong electrodynamic interaction between Ganymede's magnetosphere and the Jovian magnetospheric plasma. This is similar to the situations at the Earth and Jupiter, where the magnetospheres and auroral ovals are compressed upstream and stretched out downstream by the solar wind. This behavior is qualitatively consistent with the plasma interaction scenarios described by *Neubauer* [1998, Figure 12] and *Kivelson et al.* [2004, Figure 21.4]. It is also consistent

with the recent MHD modeling by *Jia et al.* [2008, 2009], which we discuss in further detail below.

[15] The auroral emission pattern is also not symmetric with respect to the plasma flow direction. This is most readily apparent in the polar projections of Figure 3 and is much more obvious in the northern hemisphere than the southern hemisphere. If the emission were symmetric about the plasma flow axis (X axis, dark line, in the polar projections), the oval would occur at approximately the same latitude at longitudes equidistant from the axis of symmetry, e.g., at longitudes of 0° and 180°; at 30° and 150°; at 60° and 120°, etc. Although the paucity of data and the gap in coverage between 180°W and 270°W preclude a strong conclusion, in the northern hemisphere the axis of symmetry appears to be somewhere between 300°/120° and 315°/135°, i.e., rotated from 270°/90°W toward the sub-anti-Jupiter plane, that is, from the X axis toward the Y axis. *Kivelson et al.* [2002] found that the Ganymede magnetic pole is tilted 4° from the spin axis and points toward 156°W in the north and 336°W in the south. Thus, the axis of symmetry of the Ganymede auroral oval in the northern hemisphere appears to be at least *roughly* aligned with the Ganymede magnetic axis. By contrast, in the southern hemisphere, the nominal oval appears to be much more nearly symmetric about the X (plasma flow) axis, perhaps somewhat skewed toward the $+Y$ (Jupiter) direction, but again the paucity of data and gap in coverage make this a weak conclusion.

[16] The brightnesses of the peak emission regions in each of the composite images are given in Table 2. The brightest regions in the 1998, 2003, and 2007 images have similar values (~220–260 R), but the brightest region in the 2000 image is significantly brighter (~430 R). There is also an interesting pattern apparent in 2000, 2003, and 2007 images, all of which show bright spots near the limbs, where the emission is brighter at the W (dusk) limb of the satellite compared to the E (dawn) limb. The brightest region for all three of these observing dates is near the northwest (NW) limb of the satellite, with a somewhat fainter region near the southwest (SW) limb, an even fainter emission near the southeast (SE) limb, and faintest to no emission near the northeast (NE) limb of the satellite. This pattern is very similar in both the 2003 and 2007 sub-Jupiter hemisphere images, which provides another indicator that the large-scale auroral emission pattern is repeatable and relatively stable (at least in a gross sense) on a multiyear time scale. It is not clear why the 2000, 2003, and 2007 images seem to show limb brightening effects with the bright spots, but the trailing hemisphere image from 1998 does not. It is also interesting to note that the central longitudes of the 2003 and 2007 images are different by about 20° and the peak brightness of the NW spot is 20° closer to the limb in one image compared to the other, i.e., the longitude of the brightest spot in the NW quadrant is at the same longitude and roughly the same latitude in both images. There is also a bright spot at approximately the same longitude and latitude in the 1998 image as well (close to the central meridian). Further observations would be needed to determine unambiguously whether there is a persistent bright spot near this longitude and latitude (~220°W–245°W, 35°N–50°N). This may just be an interesting coincidence, given how much the brightnesses of the spots can change from one image to the next for the individual images that make up the composites [*Feldman et al.*, 2000], because the brightest spots in the southern hemisphere in these same composite images do not seem to track in longitude nor do several other of the bright spots. For example, the brightest regions in the 2000 images are at the W (dusk) limb of the satellite near longitude 40°W. This same region is covered again in both the 2003 and 2007 images, but then it is much nearer to the center of the disk. In these images, there is no evidence for a bright region near ~40°W.

Table 2. Peak Brightnesses in Composite Images

	Localized Peak Brightness (R)
1998 (trailing)	260 (297°W, 55°N)
	240 (270°W, 50°N)
	230 (310°W, 38S)
	210 (350°W, 45°S)
2000 (leading)	430 (42°W, 25°N)
	420 (35°W, 25°S)
	275 (115°W, 28°S)
	268 (160°W, 27°S)
	150 (180°W, 14°N)
2003 (Jupiter-facing)	220 (302°W, 42°N)
	150 (292°W, 47°S)
	135 (27°W, 22°S)
	108 (40°W, 25°N)
2007 (Jupiter-facing)	245 (300°W, 37°N)
	185 (311°W, 49°S)
	125 (65°W, 32°S)
	105 (33°W, 28°N)
	95 (343°W, 36°N)
	95 (53°W, 22°N)

4. Comparison With Models and Polar Cap Boundary

[17] We next compare the location of the auroral oval with the location of the boundary between open and closed Ganymede magnetic field lines (OCFB, open-closed fieldline boundary), also called the "separatrix," as modeled by several different teams of researchers. The OCFB is where strong field aligned currents are expected to produce a field-aligned electric field capable of accelerating electrons, the likely excitation mechanism for the auroral emissions.

[18] *Khurana et al.* [2007] have modeled the OCFB boundary using a static superposition of the Ganymede and Jupiter magnetic fields, which does not take into account the strong electrodynamic interaction between Ganymede and the magnetospheric plasma. We compare the location of Ganymede's auroral oval with their model OCFB for three different locations of Ganymede relative to the current sheet (above, in, and below) in Figure 4. In this formulation, the latitude of the OCFB does not have the same shape and does not change significantly with longitude, no matter where Ganymede is relative to the current sheet. The static superposition model OCFB does not correspond well to the location of the brightest Ganymede UV auroral emission. In particular, it does not reproduce the high latitude of the northern emission in the northern trailing hemisphere or the low latitude of the emission in the northern leading hemisphere.

[19] *Kopp and Ip* [2002] used a resistive MHD simulation to model the magnetic field topology. We show their model OCFB location compared to the Ganymede auroral oval in Figure 5. Their OCFB has the same shape with longitude in the north and south, which can be conceptually described by simply shifting the northern OCFB curve to the south by

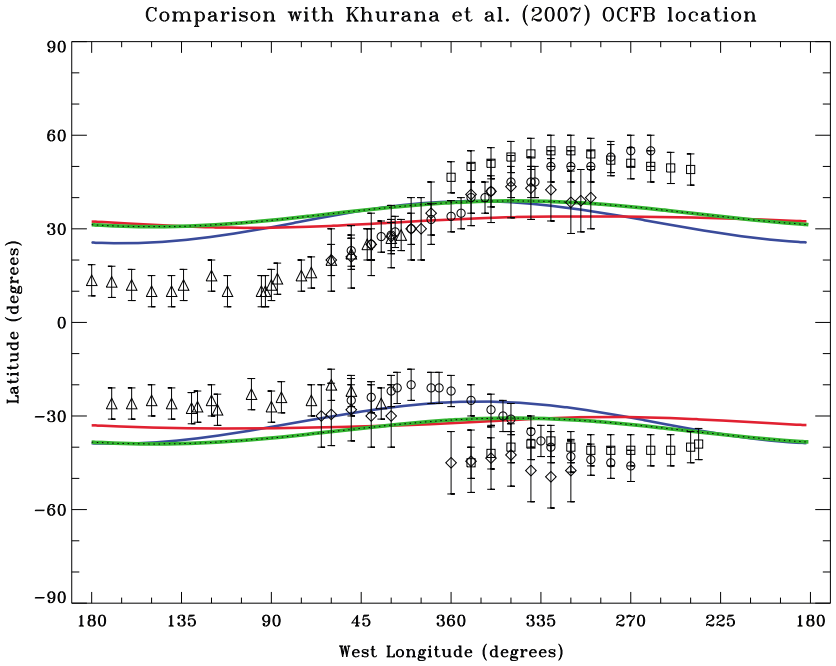

Figure 4. Comparison between the location of Ganymede's auroral oxygen emission and the *Khurana et al*. [2007] static superposition (Ganymede and Jupiter magnetic fields) model of the OCFB location. For this and subsequent figures, the red line indicates a model where Ganymede is above the current sheet, the green line where Ganymede is in or very near the current sheet, and the blue line where Ganymede is below the current sheet. The OCFB location in this model does not provide a good match to the observed location of the auroral emission.

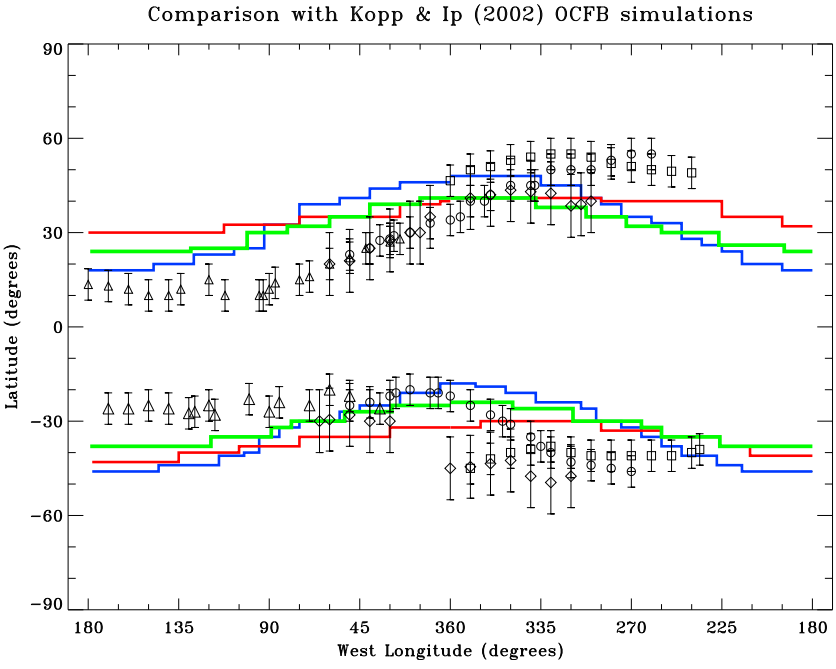

Figure 5. Comparison between the location of Ganymede's auroral oxygen emission and the *Kopp and Ip* [2002] MHD model OCFB location. The meaning of the colored lines is the same as Figure 4. This model also does not provide a good match to either the shape or location of the auroral emission.

~60° in latitude. The maximum latitude in the north corresponds to the minimum latitude in the south (at 360°W longitude), and the minimum latitude in the north corresponds to the maximum latitude in the south (at ~180°W). By contrast, the observed auroral emission pattern looks like a "butterfly diagram," with the highest latitude emission in both the north and the south occurring at the same longitude (~270°W longitude), and the lowest latitude emission in the

north and south also occurring at the same longitude of ~90°W. As shown in Figure 5, the location of the OCFB in the *Kopp and Ip* [2002] simulation does not provide a good match to the location of the auroral emission.

[20] *Paty and Winglee* [2004] used the Galileo magnetometer data to develop a 3-d multifluid simulation of the currents and fields within Ganymede's magnetosphere as well as its bulk plasma environment. Their Figure 2 compares the *Feldman et al.* [2000] trailing hemisphere image (our Figure 2c) with the temperature of each ion species, and also shows the Ganymede magnetic field line configuration. While this comparison looks promising, they do not provide quantitative information on the location of OCFB or other parameters for either the trailing hemisphere or other hemispheres, so we are not able to make a more quantitative comparison between the auroral emission and their simulations. However, recent work with updated, more sophisticated models by *Payan et al.* [2011] presented at a recent conference should allow a more quantitative comparison between these data and their models in the near future.

[21] The most sophisticated Ganymede model published to date is a three-dimensional MHD treatment by *Jia et al.* [2008, 2009]. This model has been fine-tuned to provide a close match to the ensemble of Ganymede flyby observations made by the Galileo magnetometer [*Kivelson et al.*, 1998]. The magnetic field topology resulting from this model is shown in Figure 6 for three different orientations of the background Jovian magnetic field (rows a, b, and c represent Ganymede's location above, in and below the plasma sheet, respectively) and three different vantage points (columns 1, 2, and 3 show view points from downstream, Jupiter, and upstream, respectively) that correspond to the three different hemispheres of Ganymede captured in the UV images. Figure 7 shows a comparison between the location of the OCFB from the Jia model compared to the auroral emission pattern. In addition to the OCFB location, the location of the maximum plasma thermal energy flux is also shown. While there is still somewhat of a mismatch between the data and the OCFB and energy flux patterns especially for the leading, northern hemisphere, these models clearly provide a much better fit to the data and, in particular, reproduce the "butterfly diagram" shape of the observed emission morphology.

[22] Ganymede is known to have a polar cap that is brighter and bluer at visible wavelengths than the lower latitude regions [*Smith et al.*, 1979]. There has been debate about the origin of the polar cap, with thermal segregation or charged particle modification of the surface being the two leading explanations. *Khurana et al.* [2007] noted a close correspondence between their OCFB and the boundary of

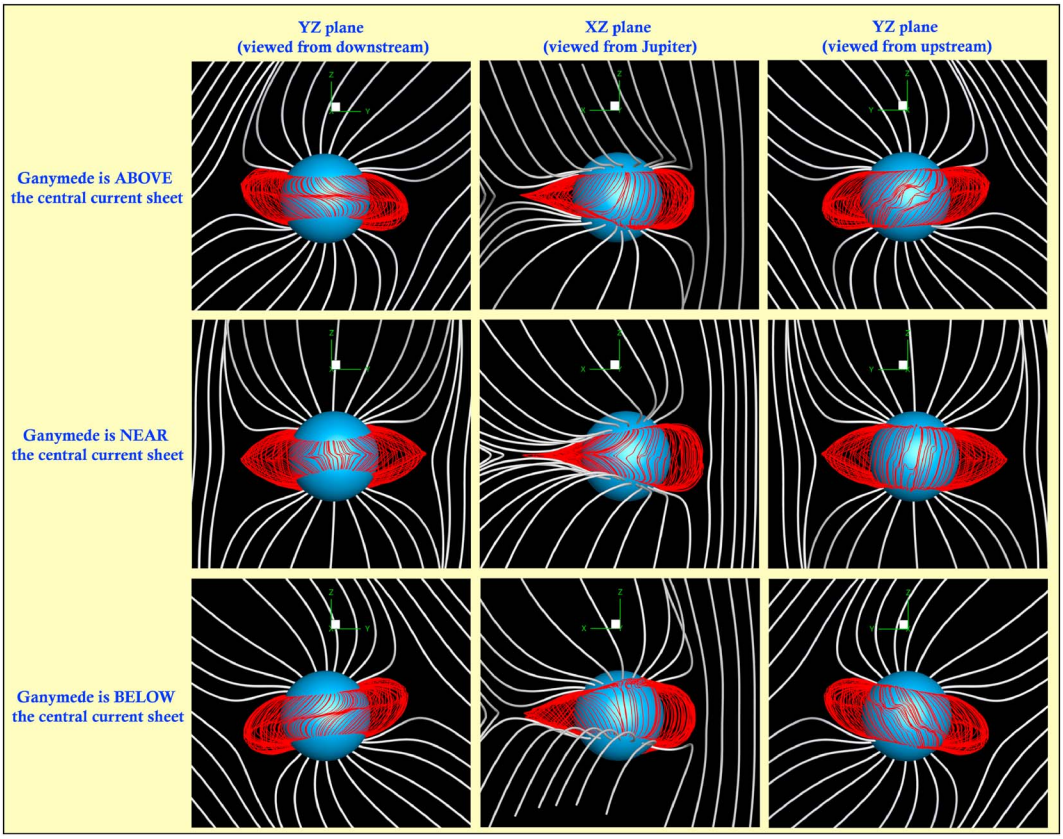

Figure 6. Magnetic field topology at Ganymede from the *Jia et al.* [2008, 2009] MHD model for three locations of Ganymede relative to the current sheet (top row: above; middle row: in; bottom row: below) and viewed from three different vantage points (left column: from downstream; middle column: from Jupiter; right column: from upstream). The three vantage points correspond to the three hemispheres of the Ganymede images shown in Figure 2. Closed (Ganymede) magnetic field lines are shown in red; open field lines are shown in white. The *XYZ* coordinate system is illustrated in Figure 1.

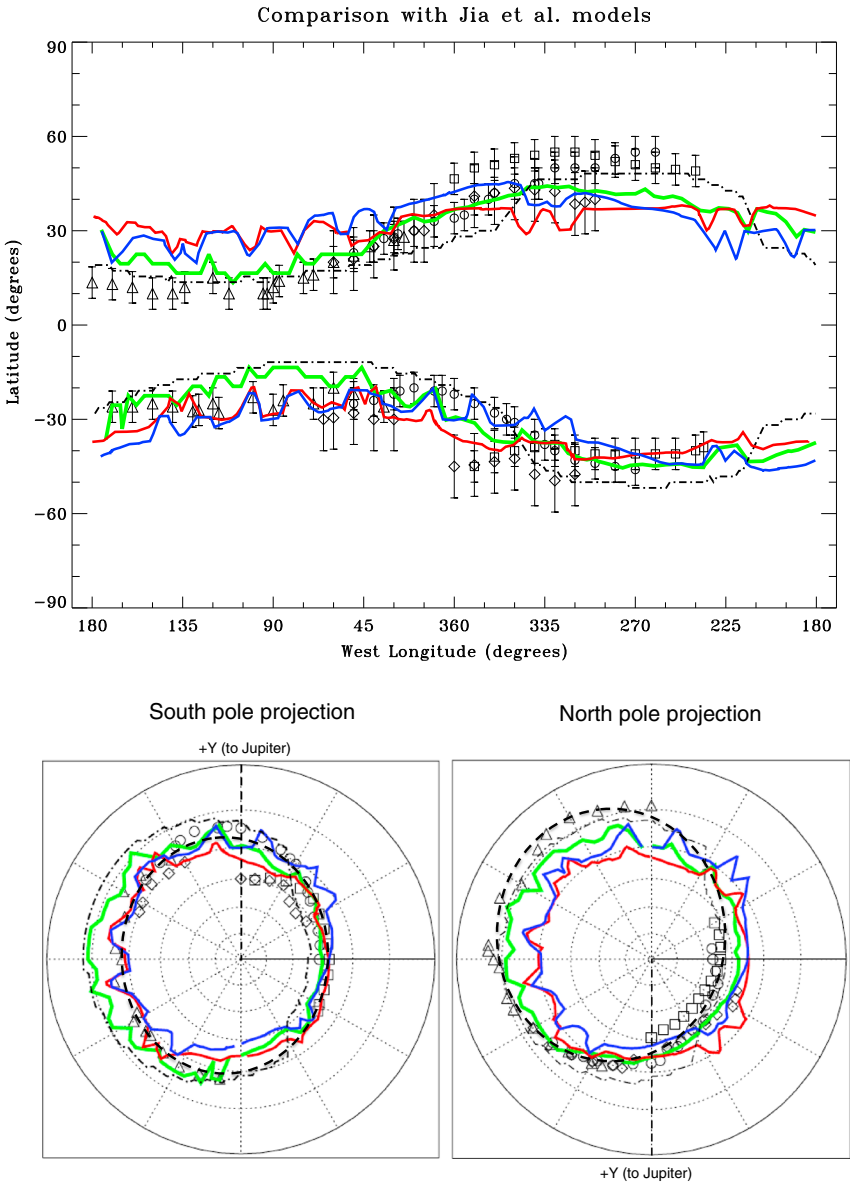

Figure 7. Comparison between the *Jia et al*. MHD model OCFB locations and the location of maximum plasma thermal energy flux from this model (black dash-dotted line). This model provides a much better match to the data than other models, correctly reproducing the overall "butterfly" shape for the location of the auroral emission. This match is very encouraging, because the model has been optimized to match the Galileo magnetometer measurements during Ganymede flybys and has not been tweaked to match the auroral emission location. The meaning of the colored lines is the same as Figure 4.

the Ganymede polar cap, which they interpreted as evidence that the polar cap is associated with charged particle effects. They also noted, using polar projection images [see *Khurana et al*., 2007, Figure 4], that a shift of their OCFB from 270°W toward 90°W longitude by 5° provided a better match to the location of the polar cap boundary. Such an empirically determined shift tends to artificially reproduce the effects of the magnetospheric interaction not included explicitly in their model, i.e., stretching of OCFB to lower latitude in the downstream direction and compressing it to higher latitude in the upstream direction. Such a shift of their OCFB would produce a more "butterfly"-like shape in the cylindrical projection plot shown in Figure 3, although given the ~20° difference between models and data, it would not result in an appreciably better fit to the auroral data. Figure 8 shows the composite Galileo SSI violet to green ratio image used by *Khurana et al*., in which the polar cap boundary is obvious (and indicated by the dark line in the figure), overlain with the auroral emission data from Figure 3. The correspondence between the two is reasonably good in the southern hemisphere, except between ~0°W and 45°W, not grossly mismatched in the northern, trailing hemisphere, but in the northern, leading hemisphere the polar cap boundary and the location of the auroral emission are not in good agreement. Because of the fact that the bright and dark regions in the higher latitudes appear to be thermally segregated, *Khurana et al*. favored the interpretation that the caps are created by higher rates of water ice sputtering at higher latitudes,

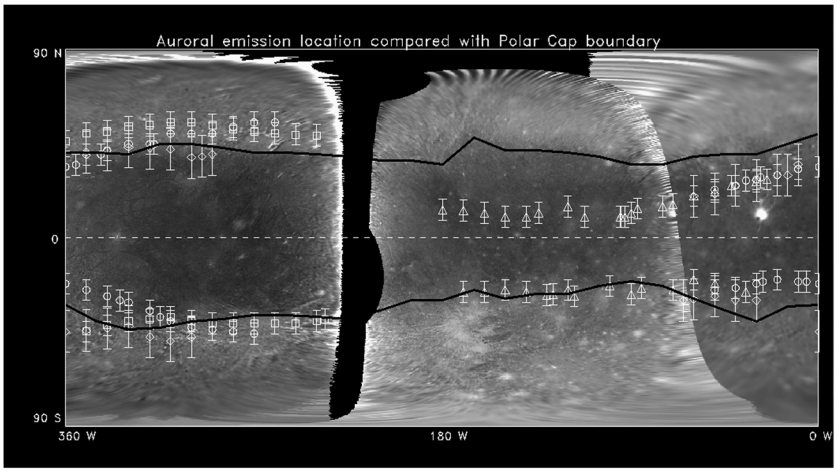

Figure 8. Comparison between the Ganymede polar cap boundary (dark line) and the Ganymede auroral emission. This is a violet-to-green filter ratio image from the Galileo SSI, identical to the image shown by *Khurana et al*. [2007, Figure 3]. The dark line is drawn at a *v*/*g* ratio = 0.84, the approximate location of the polar cap boundary. There is reasonable agreement between the two in the trailing hemisphere and the southern leading hemisphere, but there is a large mismatch in the northern leading hemisphere (0°W–180°W). This sheds some doubt on the interpretation that the polar cap is caused by charged particle precipitation in the polar regions. Note that the longitude convention has been reversed in this figure compared to earlier figures, because we are using the figure as presented previously by *Khurana et al*. [2007] for consistency.

followed by thermal segregation of the sputtered material. Sputtering at Ganymede is most efficiently accomplished by heavy ions, while the auroral emissions are generated by energetic electrons. The gyroradii of the ions are large compared to the scale of the sharp polar cap boundary. However, the dynamics of energetic ions in Ganymede's magnetic field environment is complex and warrants further study but is beyond the scope of this paper. The differences between the ion and electron behaviors (e.g., bounce times and gyroradius) may play some role in our lack of understanding of the polar cap boundary compared with the OCFB and the auroral emission location. This is clearly a complex problem, for which a good understanding still seems to require further data and modeling.

5. Discussion

[23] The close correspondence between the location of the Ganymede auroral oval and the OCFB from the *Jia et al*. model of Ganymede's magnetosphere that also agrees well with the *Galileo* magnetic field and plasma flow measurements leads us to conclude that the aurora forms at or very near to the OCFB. The peak emission intensity at the oval is the region that receives the maximum particle precipitation. Of course the ultimate energy source for the required local particle acceleration is the rotation energy of Jupiter, which is tapped via the imposed corotation electric field associated with the magnetospheric plasma flow past Ganymede. The general characteristics of the oval, occurring at higher latitude in the upstream hemisphere and lower latitude in the downstream hemisphere, are consistent with the effects on a dipole magnetic field caused by the pressure of the flowing plasma [see, e.g., *Kivelson et al*., 1998, Figure 4]. Furthermore, due to the sub-Alfvenic nature of the plasma flow, both *Kivelson et al*. [1998] and *Neubauer* [1998] calculated a very high reconnection efficiency at Ganymede, which is also seen in the MHD modeling of *Jia et al*. [2010]. The role of the corotation field in the transport of energetic electrons in the magnetosphere of Ganymede has been considered by *Eviatar et al*. [2000] using a terrestrial Birkeland current model. The meridional component of the electric field is found to show a discontinuity with a magnitude sufficient to provide the required electron fluxes to produce the aurora. The existence of strong field-aligned currents are seen in the *Jia et al*. model near the OCFB, where strong flow shears between the open field lines moving downstream and the closed field lines convecting toward upstream are present [*Jia et al*., 2010, Figure 4d]. Magnetic field-aligned electric fields, which are a likely mechanism for local acceleration of electrons, commonly develop in the presence of sufficiently intense field-aligned currents.

[24] *Neubauer* [1998] discusses the Ganymede interaction case of a moderate strength internal magnetic field coupled with an atmospheric type interaction. For the simplified case of the Alfven Mach number $M_A = 0$ and the ratio of thermal to magnetic field pressure $\beta_o = 0$ he calculates an electric potential of 363 kV across the far magnetopause, which mapped down into the polar cap [*Neubauer*, 1998, equation (73)] gives a diameter for the Ganymede polar cap of $0.87R_S$ and an amplification factor for the average electric field along the diameter of the polar cap of 3.66 over the corotational electric field. The sizes of the polar caps as measured by the extent of the auroral ovals shown in Figure 3 range from ~$0.55R_S$ (southern hemisphere along the *X* direction) to $0.76R_S$ (northern hemisphere, maximum diameter along

Y direction). For the more realistic case of nonzero (but small) M_A and β_o, *Neubauer* states that, "...the detailed physics of the separatrix will lead to a dynamic region of finite width in which reconnection occurs. ...The potential distribution may be quite complex inside the broadened separatrix. The imprint of it on the atmosphere of Ganymede will lead to two narrow bands at the boundaries of the polar caps, the regions of the polar electrojets mostly due to Hall currents in the ionosphere." He also notes that "the dissipative processes in the separatrix region lead to an increasing asymmetry between the downstream side and the upstream side." Reconnection and local acceleration at the OCFB as a source of the auroral oval emission therefore seems to be consistent with the work of multiple authors [*Kivelson et al*., 1998; *Neubauer*, 1998; *Eviatar et al*., 2001; *Jia et al*., 2009].

[25] Another important characteristic of the Ganymede aurora worth noting is its "patchiness." Bright auroral spots may correspond to localized electrojets, regions with currents driven through the ionospheric resistance by parallel electric fields. As noted by *Eviatar et al*. [2001], "It is not clear that the tenuous ionosphere of Ganymede will provide the resistivity needed to maintain the field, but the spotty nature of the aurora indicates that such may be possible locally." Local electrojets such as those shown by *Neubauer* [1998, Figure 5] for the Io volcano case may be relevant. The fact that the ionosphere also seems to be localized, and not global [*Kliore et al*., 2001], seems consistent with a picture of localized electrojets associated with the OCFB.

[26] Although acceleration by magnetic field–aligned electric fields associated with strong field-aligned currents at the OCFB seems the most likely local acceleration process, the correspondence between the Ganymede auroral oval and the OCFB location from the *Jia et al*. model is certainly not perfect. As pointed out by *Eviatar et al*. [2001], on the Earth, "the correspondence between the boundaries of the UV oval emission and electron precipitation is significant but also by no means perfect, and differences can occur." On Ganymede, the *Jia et al*. OCFB matches the southern auroral oval extremely well at all longitudes but is discrepant with the northern oval, especially at the center of the upstream hemisphere (270°W) and on the downstream hemisphere from ~45°W to 180°W. Whereas in the southern hemisphere, the "above" and "below" the current sheet cases (red and blue lines in Figure 7) match the data best and the maximum energy flux location matches the data worst; the exact opposite is the case in the northern hemisphere, where the "above" and "below" the current sheet cases provide the worst match, while the maximum energy flux location provides the best match. As mentioned previously, a dipole offset is not a likely explanation, since although it might improve the fit in one region it would most likely make it worse in other regions. It is interesting to note that the correspondence between the auroral oval location and the polar cap boundary is also quite good in the southern hemisphere, just as for the correspondence with the OCFB, but is quite discrepant for the entire northern, downstream hemisphere (0°W–180°W; see Figure 8). While the reasons for the discrepancies between the auroral oval and OCFB and the auroral oval and polar cap boundary may be quite different, the fact that both mismatches are in the northern hemisphere is telling and might also mean that the causes are related. As stated above, the bright polar cap is most likely caused by ions, not electrons, and more detailed investigation of how the ions might be affected by the localized fields and currents in the polar cap region is beyond the scope of this work.

[27] Our imperfect mapping of the auroral oval as well as the small number of measurements of the magnetosphere make it difficult to better resolve these discrepancies at present. There is only one data set in the region of largest discrepancy (northern downstream hemisphere), while multiple data sets in other regions show that there is definitely variation in the location of the oval (e.g., 300°W–360° W in both the north and south). There is no coverage of the auroral emission at all from 180°W to 230°W. The images used to map the auroral oval are temporal averages and hence do not reveal changes with time or system III longitude. There are only six sets of measurements of Ganymede's magnetic field, with none covering the downstream southern hemisphere, and only one each covering the upstream northern hemisphere and southern hemisphere, respectively. It is therefore difficult to draw more detailed conclusions or construct much more sophisticated models to compare with the data.

[28] Given the lack of data, it is perhaps not surprising that there is room for improvement in our ability to model the Ganymede interaction and the Ganymede aurora. It may be that, as with Jupiter, there are Ganymede magnetic anomalies that we have yet to uncover. Whatever the eventual explanation, it is clear that studies of Ganymede's magnetic field, the interaction at Ganymede, and Ganymede's auroral emission are in their infancy and that further sets of measurements of both the magnetic field and the auroral emission are highly desirable in order to help elucidate in more detail: the magnitude and geometry of Ganymede's internal magnetic field and how it affects the interaction with the Jovian magnetospheric plasma; how the auroral emission is generated at Ganymede, especially how it changes with time and with system III longitude; and whether there is a relationship among any or all of charged particle surface modification, the polar cap, auroral emission, and the separatrix. The results shown here should prove beneficial in helping to plan the European Space Agency's planned JUICE (JUpiter ICy moons Explorer) mission, which will provide a much more in-depth study of the solar system's largest satellite and its intriguing array of phenomena.

[29] **Acknowledgments.** This work is based on observations made with the NASA/ESA Hubble Space Telescope, obtained from the Data Archive at the Space Telescope Science Institute, which is operated by the Association of Universities for Research in Astronomy, Inc., under NASA contract NAS 5-26555. These observations are associated with programs 7939, 8224, 9296, and 10871. Support for program 8224 to MMcG, PDF, and DFS was provided by NASA through a grant from the Space Telescope Science Institute. We thank N. Murphy and R. Pappalardo for providing the Galileo image shown in Figure 8 and K. Khurana for providing previously published results in digital format.

References

Eviatar, A., D. F. Strobel, B. C. Wolven, P. D. Feldman, M. A. McGrath, and D. J. Williams (2001), Excitation of the Ganymede ultraviolet aurora, *Astrophys. J.*, *555*, 1013–1019.

Eviatar, A., D. J. Williams, C. Paranicas, R. W. McEntire, B. H. Mauk, and M. G. Kivelson (2000), Trapped energetic electrons in the magnetosphere of Ganymede, *J. Geophys. Res.*, *105*, 5547.

Feldman, P. D., M. A. McGrath, D. F. Strobel, H. W. Moos, K. D. Retherford, and B. C. Wolven (2000), HST/STIS imaging of ultraviolet aurora on Ganymede, *Astrophys. J.*, *535*, 1085–1090.

Gurnett, D. A., W. S. Kurth, A. Roux, S. J. Bolton, and C. F. Kennel (1996), Evidence for a magnetosphere at Ganymede from plasma wave observations by the Galileo spacecraft, *Nature*, *384*, 535–537.

Hall, D. T., P. S. Feldman, M. A. McGrath, and D. F. Strobel (1998), The far-ultraviolet oxygen airglow of Europa and Ganymede, *Astrophys. J.*, *499*, 475–481.

Jia, X., R. J. Walker, M. G. Kivelson, K. K. Khurana, and J. A. Linker (2008), Three-dimensional MHD simulations of Ganymede's magnetosphere, *J. Geophys. Res.*, *113*, A06212, doi:10.1029/2007JA012748.

Jia, X., R. J. Walker, M. G. Kivelson, K. K. Khurana, and J. A. Linker (2009), Properties of Ganymede's magnetosphere inferred from inproved three-dimensional MHD simulations, *J. Geophys. Res.*, *114*, A09209, doi:10.1029/2009JA014375.

Jia, X., R. J. Walker, M. G. Kivelson, K. K. Khurana, and J. A. Linker (2010), Dynamics of Ganymede's magnetopause: Intermittent reconnection under steady external conditions, *J. Geophys. Res.*, *115*, A12202, doi:10.1029/2010JA015771.

Johnson, R. E., L. J. Lanzerotti, and W. L. Brown (1982), Planetary applications of ion induced erosion of condensed gas frosts, *Nucl. Inst. Meth. Phys. Res. A*, *198*, 147–158.

Khurana, K., M. G. Kivelson, V. M. Vasyliunas, N. Krupp, J. Woch, A. Lagg, B. H. Mauk, and W. S. Kurth (2004), The Configuration of Jupiter's Magnetosphere. in *Jupiter: The Planet, Satellites and Magnetosphere*, Chap. 24, edited by. F. Bagenal, T. Dowling, W. McKinnon, Cambridge University Press.

Khurana, K. K., R. T. Pappalardo, N. Murphy, and T. Denk (2007), The origin of Ganymede's polar caps, *Icarus*, *191*, 193–202, doi:10.1016/j.icarus.2007.04.022.

Kivelson, M. G., K. K. Khurana, C. T. Russell, R. J. Walker, J. Warnecke, F. V. Coroniti, C. Polanskey, D. J. Southwood, and G. Schubert (1996), Discovery of Ganymede's magnetic field by the Galileo spacecraft, *Nature*, *384*, 537–541.

Kivelson, M. G., K. K. Khurana, F. V. Coroniti, S. Joy, C. T. Russell, R. J. Wlaker, J. Warnecke, L. Bennett, and C. Polanskey (1997), The magnetic field and magnetosphere of Ganymede, *Geophys. Res. Lett.*, *24*, 2155.

Kivelson, M. G., J. Warnecke, L. Bennett, S. Joy, K. K. Khurana, J. A. Linker, C. T. Russell, R. J. Walker, and C. Polanskey (1998), Ganymede's magnetosphere: Magnetometer overview, *J. Geophys. Res.*, *103*(E9), 19,963–19,972.

Kivelson, M. G., K. K. Khurana, and M. Volwerk (2002), The Permanent and Inductive Moments of Ganymede, *Icarus*, *157*, 507-522, doi:10.1006/icar.2002.6834.

Kivelson, M. K., F. Bagenal, W. S. Kurth, F. M. Neubauer, C. Paranicas, and J. Saur (2004), Magnetospheric Interactions with Satellites, in *Jupiter: The Planet, Satellites and Magnetosphere*, chap. 21, edited by F. Bagenal, T. Dowling, W. McKinnon, Cambridge University Press.

Kliore, A., J., A. Anabtawi, A. F. Nagy, D. P. Hinson, and Galileo Radio Propagation Science Team (2001), The ionospheres of Ganymede and Callisto from *Galileo* radio occultations, *B.A.A.S.* 33, 1084.

Kopp, A., and W.-H. Ip (2002), Resistive MHD simulations of Ganymede's magnetosphere 1. Time variabilities of the magnetic field topology, *J. Geophys. Res.*, *107*(A12), 1490, doi:10.1029/2001JA005071.

McGrath M. A., E. Lellouch, D. F. Strobel, P. D. Feldman, and R. E. Johnson (2004), Satellite Atmospheres, in *Jupiter: The Planet, Satellites and Magnetosphere*, Chap. 19, edited by F. Bagenal, T. Dowling, W. McKinnon, Cambridge University Press.

Neubauer, F. M. (1998), The sub-Alfvenic interaction of the Galilean satellites with the Jovian magnetosphere, *J. Geophys. Res.*, *103*(E9), 19843–19866.

Paranicas, C., W. R. Paterson, A. F. Cheng, B. H. Mauk, R. W. McEntire, L. A. Frank, and D. J. Williams (1999), Energetic particle observations near Ganymede, *J. Geophys. Res.*, *104*, 17, 459.

Paty, C., and R. Winglee (2004), Multi-fluid simulations of Ganymede's magnetosphere, *Geophys. Res. Lett.*, *31*, L24806, doi:10.1029/2004GL021220.

Payan, A. P., C. S. Paty, K. D. Retherford, and B. Bonfond (2011), Using 3D Multi-Fluid Simulations to Investigate the Periodicity of the Auroral Brightness at Ganymede and Its Dependence on Precipitating Particle Temperatures, American Geophysical Union, Fall Meeting 2011, abstract #SM21B-2010.

Saur, J., S. Duling, L. Roth, P. D. Feldman, D. F. Strobel, K. D. Retherford, M. A. McGrath, and A. Wennmacher (2011), HST STIS Observations of Ganymede's Auroral Ovals at Eastern Elongation, American Geophysical Union, Fall Meeting 2011, abstract #SM23D-08.

Scudder, J. D., E. C. Sittler, and H. S. Bridge (1981), A survey of the plasma electron environment of Jupiter - a view from Voyager, *J. Geophys. Res.*, *86*, 8167.

Smith, B. A., et al. (1979), Galilean satellites and Jupiter—Voyager 2 imaging science results, *Science*, *206*, 927–950.

Williams, D. J., B. H. Mauk, and R. W. McEntire (1997a), Trapped electrons in Ganymede's magnetic field, *Geophys. Res. Lett.*, *24*, 2953.

Williams D. J., B. H. Mauk, R. W. McEntire, E. C. Roelof, T. P. Armstrong, B. Wilken, J. G. Roederer, S. M. Krimigis, T. A. Fritz, L. J. Lanzerotti, and N. Murphy (1997b), Energetic particle signatures at Ganymede: Implications for Ganymede's magnetic field, *Geophys. Res. Lett.*, *24*, 2163.